

SYNTHESIS, CHARACTERIZATION, ANTIBACTERIAL AND CYTOTOXIC EFFECTS OF SILVER NANOPARTICLES

G. M. SULAIMAN^{a*}, E. H. ALI^a, I. I. JABBAR^b, A. H. SALEEM^a

^a *Biotechnology Division, Applied Science Department, University of Technology, Baghdad, Iraq*

^b *Applied chemistry Division, Applied Science Department, University of Technology, Baghdad, Iraq*

To investigate the biomedical potential of silver nanoparticles prepared by reduction of silver ions with ascorbic acid in the presence of the stabilizer Daxad on different pathogenic bacteria and toxicity against human acute promyelocytic leukemia (HL-60) cell line were performed. Characterization using UV-VIS spectrophotometry and X-ray diffraction analysis were used. Antimicrobial activity against five bacterial strains was tested using disc diffusion method and by agar plate and broth medium methods. While, cytotoxicity test using MTT was obtained on the human leukemia cell line (HL-60). UV-Vis spectral analysis showed silver surface plasmon resonance band at 425 nm. X-ray diffraction showed that the particles were crystalline in nature with face centered cubic structure of the bulk silver with broad peaks at 38.56° and 44.81°. In conclusion, the synthesized silver nanoparticles efficiently inhibited the growth of pathogenic bacteria and reduce viability of the HL-60 cells in a dose-dependent manner. Further studies should be given special attention for anticancer potentials while warranting for toxicity against normal cells is needed.

(Received March 28, 2014; Accepted June 2, 2014)

Keywords: Silver Nanoparticles; Daxad; Antibacterial activity; Cytotoxic effect.

1. Introduction

Nanosized inorganic particles, of either simple or composite nature, display unique physical and chemical properties and represent an increasingly important material in the development of novel nanodevices which can be used in numerous physical, biological, biomedical, and pharmaceutical applications [1- 4]. A number of investigators offer the possibility of generating new types of nanostructured materials with designed surface and structural properties [5-7]. The preparation of uniform nanosized drug particles with specific requirements in terms of size, shape, and physical and chemical properties is of great interest in the formulation of new pharmaceutical products [3,6,8,9]. One nanoparticle with possible use in biomedical applications is silver (Ag). Nano-silver possesses a high extinction coefficient, high surface plasmon resonance and anti-microbial properties which are less toxic than the bulk form [10]. Silver nanomaterials have shown a variety of uses in everyday consumer's lives such as: nanosilver infused storage containers, nanosilver coated surfaces of medical devices to reduce hospital related infections, bandages, footwear, and countless household items which claim to be anti-microbial [11-14]. Silver nanoparticles is a popular additive in many health products as listed above due to its unique ability to fight infectious diseases, slow the growth of bacterium, mold and germs [15]. Because silver compounds have been used as antimicrobial compounds in various biomedical products and applications, several investigators have begun evaluating the use of silver nanoparticles as anti-cancer [16-18].

*Corresponding author: gmsbiotech@hotmail.com

While all of these properties appear to make nanosilver the new “wonder-drug” of the nanotechnology world, problems arise. Therefore, the present work was designed to explore the antimicrobial activity of the silver nanoparticles, this potential activity of the silver nanoparticles was evaluated by agar plate and broth medium methods with Gram-negative bacteria, Gram-positive bacteria and toxicity against human acute promyelocytic leukemia (HL-60) cell line were also evaluated.

2. Materials and Methods

2.1 Materials

The chemical silver nitrate (AgNO_3), Mueller-Hinton agar (MHA) were purchased from Merck, Germany. Penicillin and streptomycin were purchased from Bio Source International, Belgium. Tissue culture plastic wares were obtained from BD Bioscience (USA). All organic solvents used were of HPLC grade. RPMI 1640, fetal bovine serum (FBS) and MTT (3-(4, 5-Dimethyl-thiazol-2-yl)-2, S-diphenyltetrazolium bromide) were purchased from Sigma Chemical Co. (St. Louis, MO, USA).

2.2 Synthesis of Daxad

Daxad used in the present study was synthesized, following a procedure reported in the literature of Yoshio et al. [19] and shown in Fig 1. At first, 95% naphthalene was melted in a glass flask equipped with reflux condenser, and then 98% H_2SO_4 was dipped into the flask in the mole ratio of 1-1.05 (naphthalene to H_2SO_4). The temperature of the flask was kept under 115°C during the course of H_2SO_4 addition. After the addition of H_2SO_4 , the flask was heated at 150°C for 3 h and the sulfonation of naphthalene took place. After the sulfonation, the unreacted naphthalene and the resultant water were get rid of by reduced pressure distillation. Then formaldehyde was dipped into the flask in the mole ratio of 1-1.05 (naphthalene to formaldehyde) and the temperature was kept under 105°C . After that, the flask was held at this temperature for over 6 h and the condensation reaction proceeded. With the progress of condensation, the viscosity of the product in the flask increased and the stirring became difficult. Hot water was added into the flask to make the stirring easy. The material is then condensed with formaldehyde and the polymerised naphthalene sulfonic acid molecule is neutralized by sodium. The neutralization product was passed through the filter paper, and then was used in preparation of silver nanoparticles.

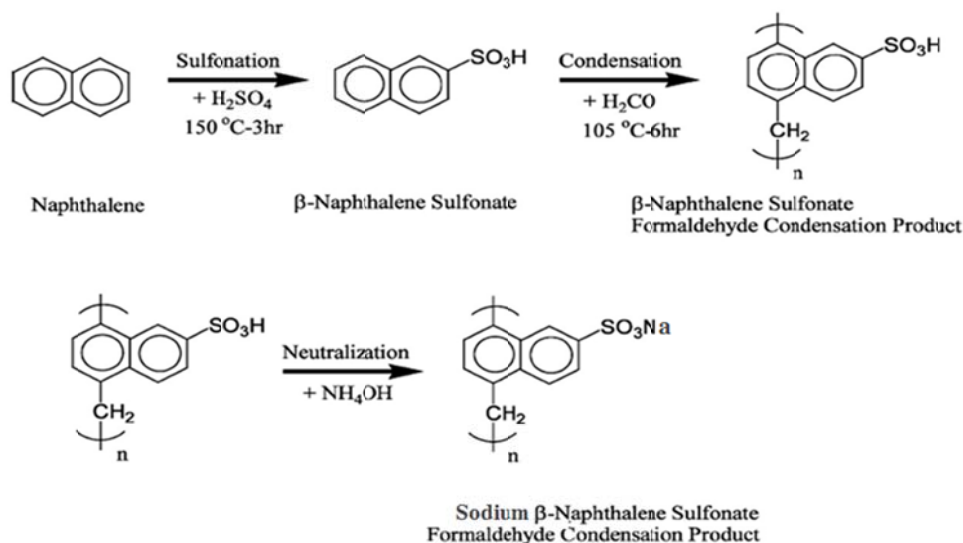
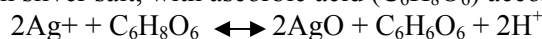


Fig.1. Process Process of the Daxad synthesis [19].

2.3 Preparation of Silver Nanoparticles

The silver nanoparticles were prepared following the procedure described previously [4]. Slight modifications were made in order to obtain an aqueous solution of silver nanoparticles. An easy chemical way to obtain nanostructured silver particles is by reduction, in aqueous solution, of Ag NO₃, the most common silver salt, with ascorbic acid (C₆H₈O₆) according to equation.



However, the silver nanoparticles were prepared by adding, under agitation, 10 mL of an aqueous 1 mM ascorbic acid solution at a flow rate of 3 mL min⁻¹ into 90 mL of an aqueous solution containing 5 wt% of Daxad and 1 mM AgNO₃. The reacting solutions were agitated with a stirrer at 900 rpm at room temperature. To remove the surfactant and excess silver ions, the resulting silver precipitate was washed five times with deionized water.

2.4 Characterization of Silver Nanoparticles

UV-Vis spectral analysis was done by using UV-Vis spectrophotometer (PG- T80⁺ UV/Vis spectrophotometer, England) from 300-600 nm at a resolution of 1 nm. XRD measurements of the silver nanoparticles solution drop-coated on glass were done on a Shimadzu XRD-6000 model with 40 kv, 30 mA with Cu k α radiation at 2 θ angle. X-ray powder diffraction is a rapid analytical technique primarily used for phase identification of a crystalline material and can provide information on unit cell dimensions. The crystallite domain size was calculated from the width of the XRD peaks, assuming that they are free from non-uniform strains, using the Scherrer formula.

$$D = 0.94 \lambda / \beta \cos \theta$$

2.5 Fourier Transform Infrared (FTIR) Spectroscopy Measurement

Sample of the aqueous solution of the silver nanoparticles were prepared by using centrifugation and suspended with phosphate buffer and analyses done by FTIR. Sample was measured by FTIR 8400S spectrometer in attenuated total reflection mode and using spectral range of 4000-500 cm⁻¹ with resolution of 4 cm⁻¹.

2.6 Evaluation of Antibacterial Activity

The silver nanoparticles synthesized using Daxad was tested for antimicrobial activity by agar well diffusion method against different pathogenic microorganisms *Escherichia coli*, *Pseudomonas aeruginosa*, *Proteus vulgaris*, *Klebsiella pneumoniae* (Gram Negative), and *Staphylococcus aureus* (Gram Positive). The pure cultures of bacteria were subcultured on MHA. Each strain was swabbed uniformly onto the individual plates using sterile cotton swabs. Wells of 8 mm diameter were made on nutrient agar plates using gel puncture. Using a micropipette, 50 μL of nanoparticle solution was poured onto each well on all plates. After incubation at 37°C for 24 hours, the diameter of zone inhibition was measured in millimeter, and was recorded as mean ± SD of the triplicate experiment. While, the bacterial suspension was prepared and adjusted by comparison against 0.5 Mc-Farland turbidity standard (5 × 10⁸ cell ml⁻¹) tubes. All bacteria strains were sub-culture on nutrient broth. The broth was inoculated with 0.2 ml of bacterial strains, then 1 ml of 0.5 or 1 mM of silvernanoparticles were added. The tubes were incubated at 37 °C for 24 h. The growth of control bacterial growth was measured by turbidity at 600 nm wavelength.

2.7 Viability of HL-60 Cell Line

The HL-60 cell line was cultured in RPMI-1640 medium supplemented with 10% heat-inactivated foetal bovine serum (FBS), 2 mM L-glutamine and 100U/mL penicillin–streptomycin in a humidified atmosphere of 5% CO₂ at 37 °C in in 96 – well flat-bottom culture plates. After 48 h in exponentially growing phase, the cells were treated with either 0.5 or 1 mM of silvernanoparticles for 24 h. Then, the cell viability was evaluated by the MTT colorimetric technique. Briefly, 100 μl of the yellow tetrazolium MTT (3-(4, 5-dimethylthiazolyl-2)-2, 5-diphenyltetrazolium bromide) without phenol red, are yellowish in color solution (5 mg mL⁻¹ in PBS) was added to each well. The plates were incubated for 3-4 h at 37 °C, for reduction of MTT

by metabolically active cells, in part by the action of dehydrogenase enzymes, to generate reducing equivalents such as NADH and NADPH. The resulting intracellular purple formazan solubilized the MTT crystals by adding and quantified by spectrophotometric mean and then the supernatants were removed. For solubilization of the MTT crystals, 100 μ L of isopropanol or DMSO was added to the wells. The plates were placed on a shaker for 15 min for complete solubilization of crystals and then the optical density of each well was determined. The quantity of formazan product as measured by the amount of 545 nm absorbance is directly proportional to the number of living cells in culture [17]. Each experiment was done in triplicate. The relative cell viability (%) related to control wells containing cell culture medium without nanoparticles as a vehicle was calculated as follow:

$$\text{Percentage of cell viability (\%)} = \left(\frac{\text{Sample Absorbance}}{\text{Control Absorbance}} \right) \times 100$$

2.8 Statistical analysis

The grouped data were statistically evaluated using ANOVA with SPSS/14 software. Values are presented as the mean \pm S.D. of the three replicates of each experiment.

3. Results

As shown in Fig. 2, the color of AgNO_3 suspensions through different washing times and the color was changed from dark yellow, (E) to yellow (B and C), and finally light yellow (D). The evaluation of silver nanoparticles was confirmed at several times intervals using UV-Vis spectral analysis and showed silver surface plasmon resonance band at 425 nm (Fig. 3).

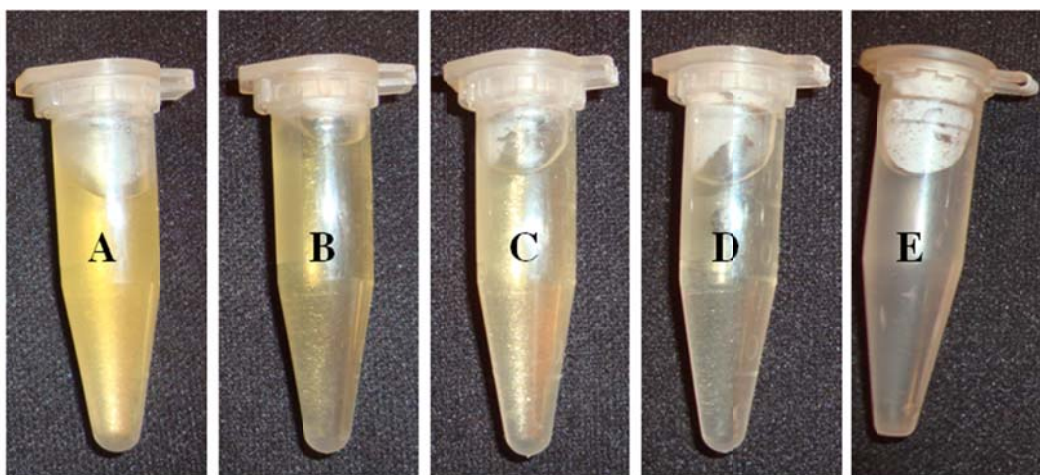


Fig.2. Photograph showing stages of silver nanoparticles before washing (A) and after washing (B) two times (C) three times (D) five times as compared with 1 mM AgNO_3 (E).

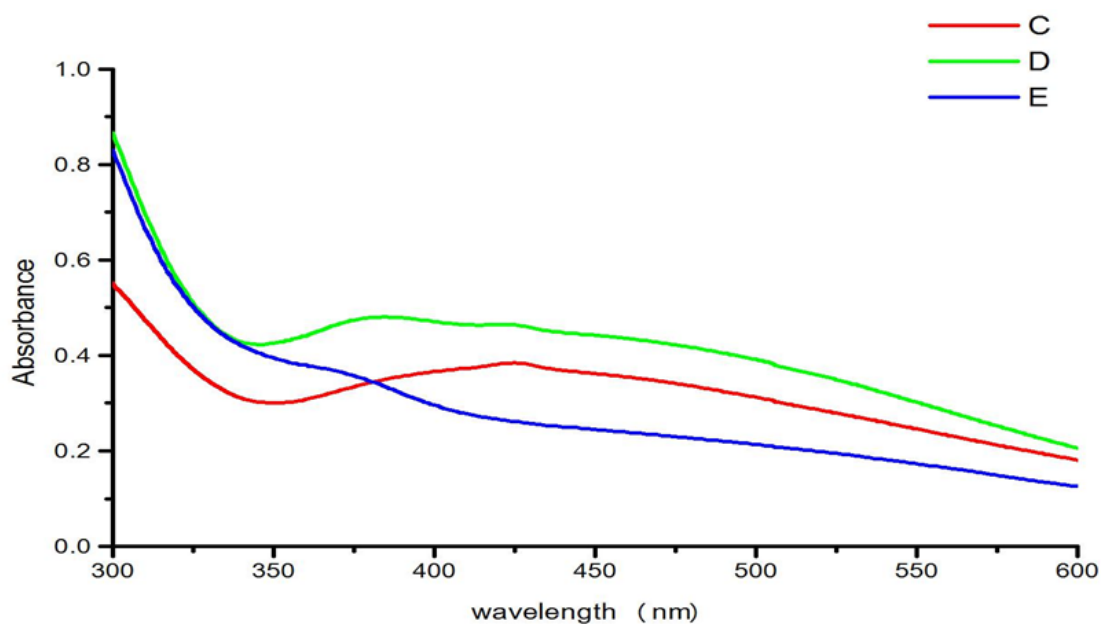


Fig.3. UV/Vis absorption spectra evaluations of silver nanoparticles (Sample D, Figure 1) after (E) 3 min (D) 6 min (C) 10 min of reaction.

The X-ray diffraction pattern of the biosynthesized silver nanostructure was further demonstrated and confirmed by the characteristic peaks observed in the XRD image (Fig. 4). The XRD pattern showed two intense peaks (38.56° and 44.81°) in the whole spectrum of 2θ value ranging from 20 to 50 and indicated that the structure of silver nanoparticles is face-centered cubic (fcc). These are corresponding to (111) and (200) planes for silver, respectively. The lattice constant calculated from this pattern was $a = 4.086 \text{ \AA}$ and the data obtained was matched with the database of Joint Committee on Powder Diffraction Standards (JCPDS) file No. 04-0783. The average grain size of the silver nanoparticles formed in the bioreduction process was determined using Scherrer's formula and was estimated as 30 nm.

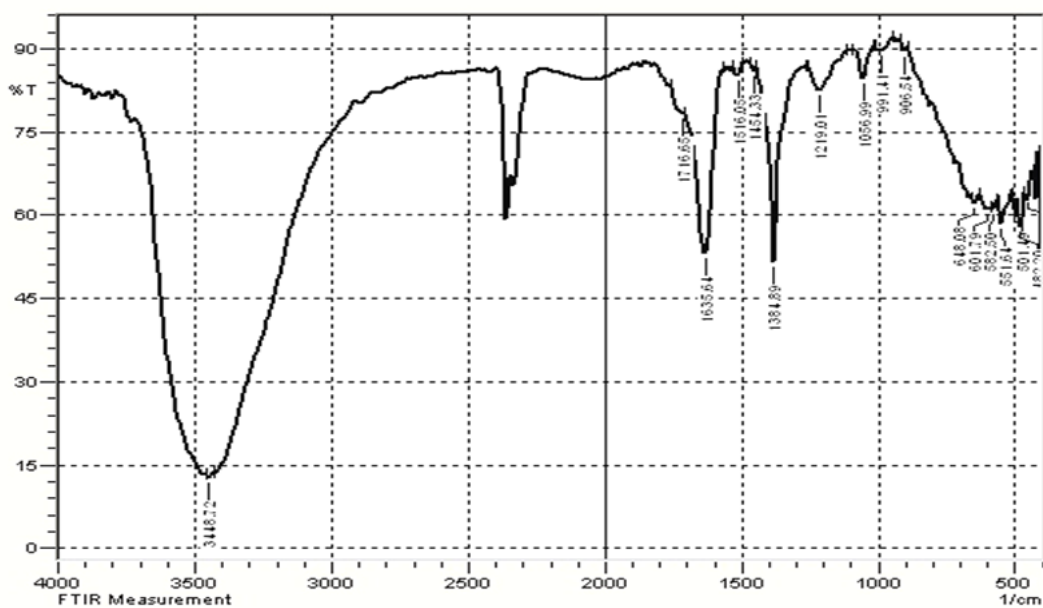


Fig.4. FTIR spectra of silver nanoparticles synthesized using Daxad.

The FTIR spectrum of Ag nanoparticle show absorption peaks at 1635 cm^{-1} and peaks at 1219 cm^{-1} , which can be ascribed to the C=C double bond and C–H bending, The FT-IR spectrum of sample (Fig. 4) shows an absorption at 2264 cm^{-1} assigned to the stretching vibration of the $\text{C}\equiv\text{N}$ group of AgCN. The strong bond in the region 3448 cm^{-1} was identified due to O–H stretching. While, the peak at 2360 cm^{-1} was attributed to carbon dioxide.

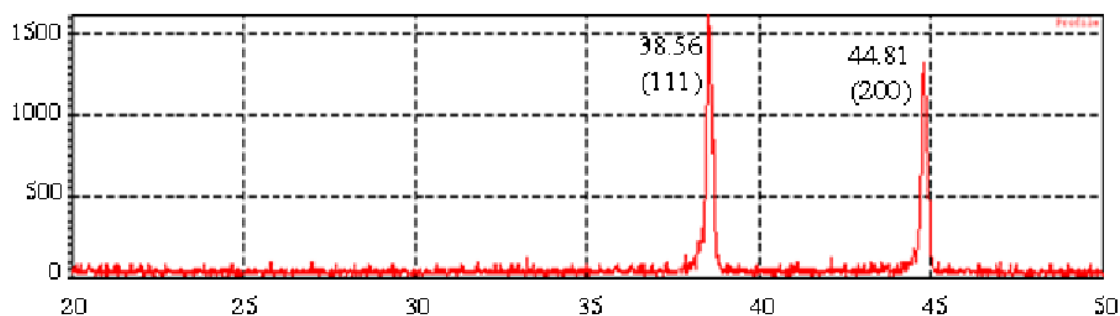


Fig.5. XRD patterns recorded from drop-coated films on glass substrate of silver nanoparticles synthesized by daxad with AgNO_3 aqueous solutions.

The antimicrobial activity of silver nanoparticles against various pathogens including Gram positive and negative bacteria was investigated by agar plate and broth medium methods. As shown in figure 6, the diameters of inhibition zones increased for all the tested bacteria after treatment with 0.5 mM or 1 mM of AgNPs and showed effect with dose dependant manner.

For the medium growth test, number of bacteria was determined by recording the bacterial optical density. UV-VIS spectrophotometer was used in the measurements of the optical density of the bacterial cultures in liquid nutrient medium, with the measuring wavelength set at 600 nm. Based on the data derived from the liquid medium tests, we were able to see that the bacterial cell number was dropped tremendously in both types of tests and the inhibition was concentration dependant manner (figures 7 and 8).

The in vitro cytotoxic effects of silver nanoparticles were screened against HL-60 cell line and viability of tumor cells was confirmed using MTT assay. The silver nanoparticles were able to reduce viability of the HL-60 cells in a dose-dependent manner as shown in (Table 1). The exposures to AgNPs resulted in toxicity to the HL-60 cells and reached to 60 % and 83% dead cells after 24 h of treatment with 0.5 mM or 1 mM of AgNPs, respectively. However, the toxicity of AgNPs appeared much higher than that of AgNO_3 alone (20%) at the same period of incubation (Table 1).

Table 1. Percent viability measured on HL-60 cells after treatment with silver nanoparticles for 24 h, by MTT assay. The data are expressed as Mean \pm Standard Deviation (SD) of three independent experiments.

Treatment	Time of incubation	
	24 hours	
	Dead (%)	Viable (%)
HL-60 + RPMI	2 ± 0.16	98
HL-60 + AgNO_3	20 ± 1.86	80
HL-60 + 0.5 mM AgNPs*	60 ± 3.40	40
HL-60 + 1mM AgNPs	83 ± 5.38	17

* AgNPs = Silver nanoparticles

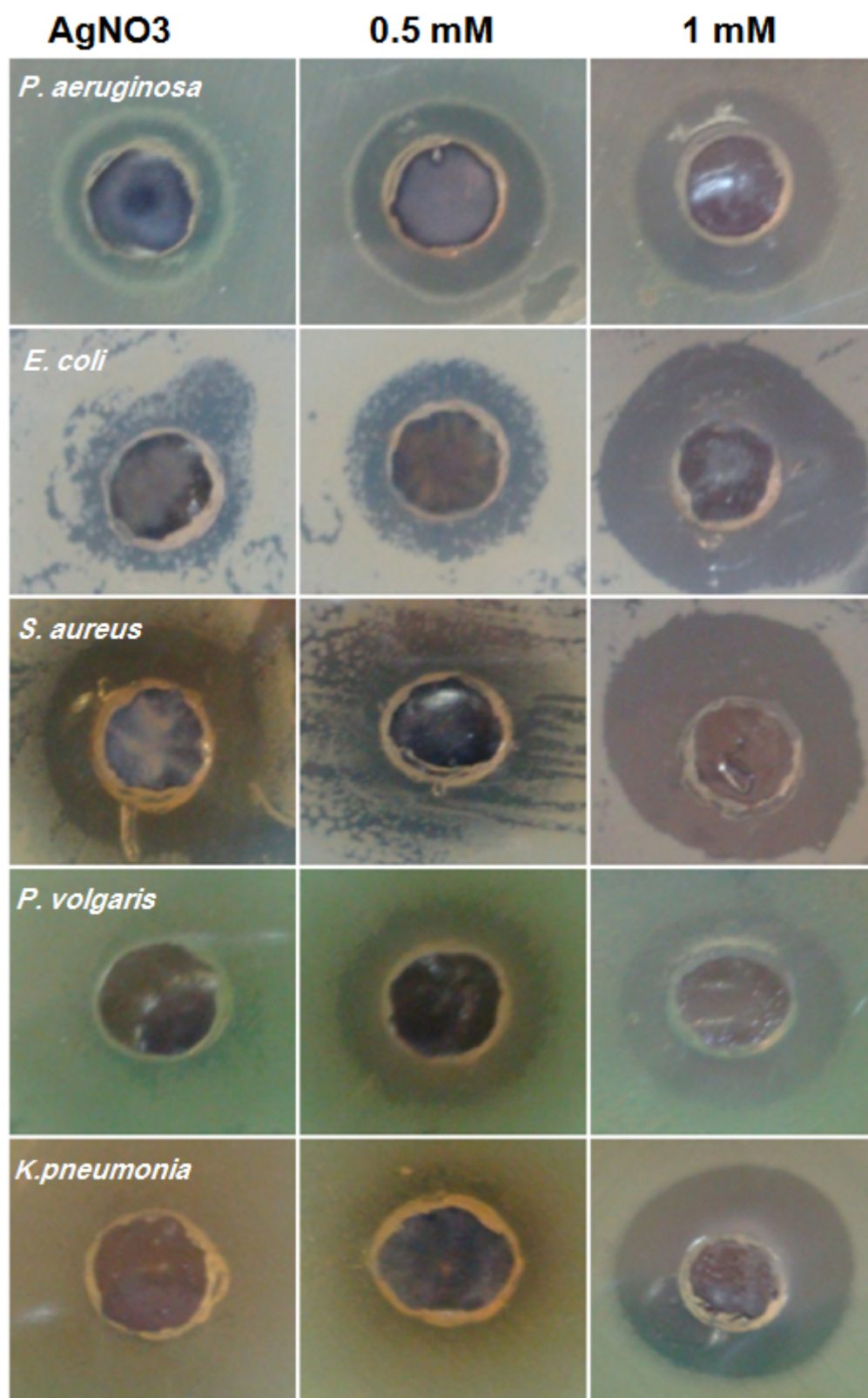


Fig.6. Antibacterial activity assay against Gram negative and positive bacteria treated with AgNO₃, 0.5 mM AgNPs and 1 mM AgNPs.

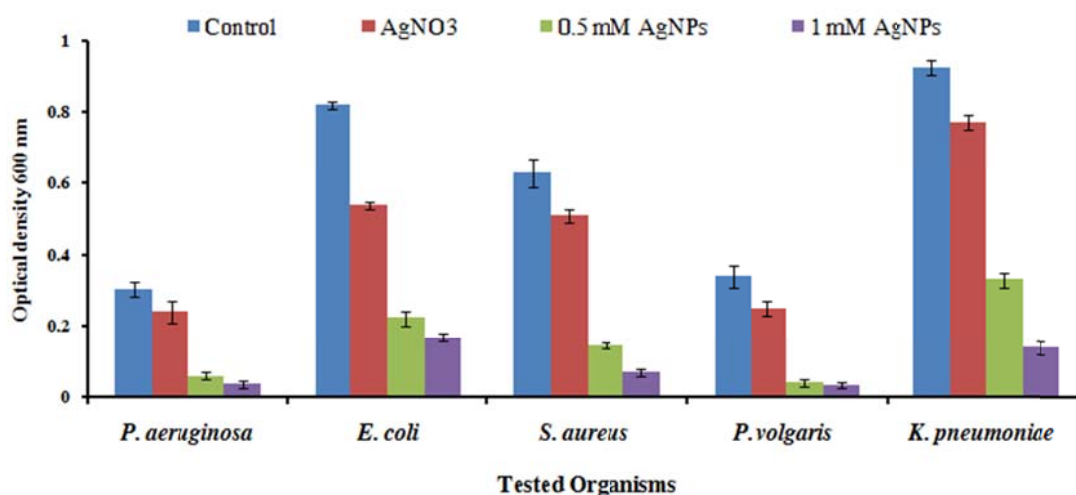


Fig.7. Optical density of tested bacteria treated with silver nanoparticles.

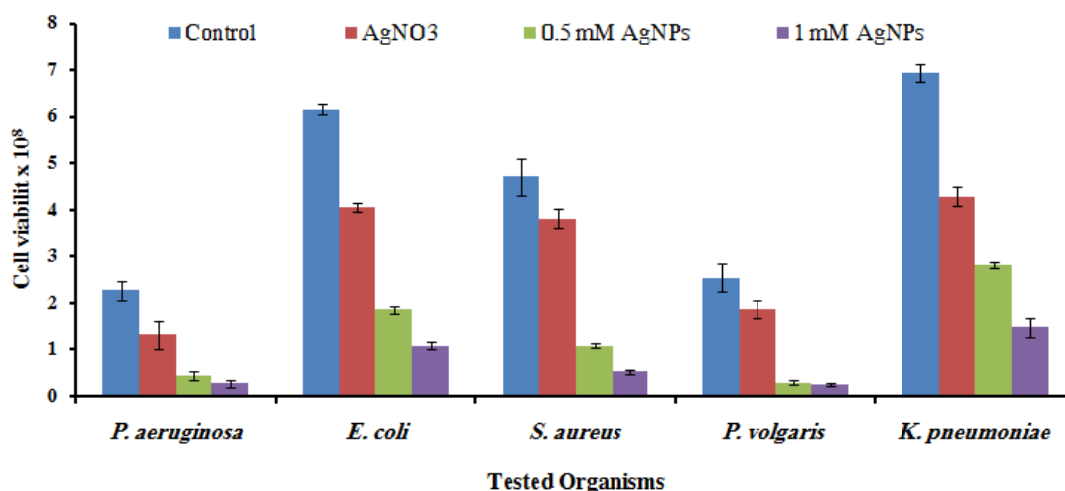


Fig.8. Effect of silver nanoparticles against cell viability of tested bacteria

4. Discussion

This study has demonstrated that stable dispersions of silver nanoparticles can be rapidly prepared by reduction of silver ions with ascorbic acid in the presence of the stabilizer Daxad. This revealed a characteristic peak for AgNPs at 425 nm, which confirmed the formation of the silver nanoparticles. The frequency and width of the surface plasmon absorption depends on the size and shape of the metal nanoparticles as well as on the dielectric constant of the metal itself and the surrounding medium [20,21]. When the plasmon peak shifts toward shorter wavelengths (blue shift) from 425 to 415 nm, meaning a decrease of the particle size, while the rise to a red shift from 425 to 440 nm, meaning that the particle size increases and large silver aggregates have been formed [22,23]. The figure also indicates that the surface plasmon absorption peaks of the AgNPs are centered, implying that the AgNPs were mainly spheroidal and that their surface plasmon absorption spectra broadened with the increase of the initial AgNO₃ concentration [24]. It is generally recognized that UV–VIS spectroscopy could be used to examine size- and shape-controlled nanoparticles in aqueous suspensions [21].

In present study the X-ray pattern of synthesized silver nanoparticles matches the FCC structure of the bulk silver and there was no obvious other phases as impurities were found in the XRD patterns, and it can be stated that the obtained silver nanoparticles had a high purity. The X-ray diffraction results clearly show that the silver nanoparticles formed by the reduction of Ag⁺ ions with ascorbic acid in the presence of daxad are crystalline in nature [25,26]. In order to avoid

particle agglomeration and maintain a good dispersion in water, a dispersing agent is usually employed. Daxad, a polymer formed by the condensation of naphthalene sulfonic acid with formaldehyde, is a good dispersing agent for silver particles, even in very strong acidic conditions where the reduction of Ag^+ is slowed down due to the decrease of the double-deprotonated ascorbate anion, ascorbate. Being a stronger reducing agent than ascorbic acid, it is responsible for reduction in basic and neutral conditions [27]. Silver particles are thermally unstable in the reaction solution. By increasing the temperature to 100 C, they dissolve because the nitrate groups, in strong acidic conditions, oxidize AgO to Ag^+ forming nitrogen oxides. The Ag^+ ions probably remain on the Daxad, due to the presence of the coordinating sulfonic groups. Nitrogen oxide then reacts with dehydroascorbate, probably forming as an intermediate O-nitrosoascorbate. In turn, nitrosoascorbate decomposes into erythro-ascorbate and cyanides, perceptible by the characteristic smell [28].

FT-IR absorption spectra can provide the information about the chemical change of the functional groups involved in bioreduction. However, the FTIR spectrum of the present study is clearly indicated that the dispersant adsorbs on the surface of silver particles. The spectra are characterized by the aromatic $\text{C}=\text{C}$ stretching vibrations between 1381 and 1635 cm^{-1} and symmetric and asymmetric stretching of the sodium sulfonate groups between 1056 and 1219 cm^{-1} . The CN groups further increase the Ag^+ -polymer interactions, forming $-\text{Ag}-\text{C}\equiv\text{N}-\text{Ag}-\text{C}\equiv\text{N}-$ linear chains parallel to the long direction of the polymer they might be due to the presence on the polymer of AgCN chains [29].

In this study, the application of silver nanoparticles as an antibacterial agent was investigated and exhibited better antibacterial activity against all tested bacteria. It appears that these particles could have an excellent biocidal effect and effectiveness in reducing bacterial growth for practical applications such as the formulation of various biocidal materials. The mechanism of inhibitory action of silver nanoparticles on microorganisms is not very well-known [30,31]. However, several mechanisms have been proposed to explain the inhibitory effect of silver nanoparticles on bacteria. It is assumed that the high affinity of silver towards sulfur and phosphorus is the key element of the antimicrobial effect. Due to the abundance of sulfur-containing proteins on the bacterial cell membrane, silver nanoparticles can react with sulfur-containing amino acids inside or outside the cell membrane, which in turn affects bacterial cell viability. It was also suggested that silver ions (particularly Ag^+) released from silver nanoparticles can interact with phosphorus moieties in DNA, resulting in inactivation of DNA replication, or reacting with sulfur-containing proteins, leading to the inhibition of enzyme functions which results in loss of cell viability and eventually resulting in cell death [32,33].

In this study, we have employed a dose dependent approach to evaluate the toxicity of the nanoparticles on human acute promyelocytic leukemia (HL-60). The viability of HL-60 cells considerably decreased with increasing doses of incubation. The mortality data obtained in these results allow us to predict their potential not only because of the cytotoxic effect, but also in terms of the potential for tumor reduction. The cytotoxic effects of silver are the result of active physicochemical interaction of silver atoms with the functional groups of intracellular proteins, as well as with the nitrogen bases and phosphate groups in DNA [17, 34].

5. Conclusion

The biosynthesized silver nanoparticles showed excellent antimicrobial activity and possessed considerable cytotoxic effect against HL-60 *in vitro*. Therefore, further studies must be conducted to fully characterize the mechanisms of toxicity of these particles and to examine anticancer potentials for other cases. Hence it is imperative that the biological applications employing silver nanoparticles should be given special attention for anticancer potentials while warranting for toxicity against normal cells is needed.

References

- [1] W.C. Chan, D.J. Maxwell, X. Gao, R.E. Bailey, M. Han, S. Nie, *Curr Opin Biotechnol.* **13**, 40 (2002).
- [2] I. Brigger, C. Dubernet, P. Couvreur, *Adv. Drug Delivery Rev.* **54**, 631 (2002).
- [3] X Wu, H Liu, J Liu, K.N. Haley, J. A. Treadway, J. P. Larson, N. Ge , F. Peale M.P. Bruchez, *Nat. Biotechnol.* **21**, 41 (2003).
- [4] I. Sondi and B. Salopek-Sondi, *J. Colloid Interface Sci.* **275**, 177 (2004).
- [5] H. Mattoussi, J. M. Mauro, E. R. Goldman, G. P. Anderson, V. C. Sundar, F. V. Mikulec, M. G. Bawendi, *J. Am. Chem. Soc.* **122**, 12142 (2000).
- [6] L. Joguet, I. Sondi, E. Matijevic, *J. Colloid Interface Sci.* **251**, 284 (2002).
- [7] I. Sondi, T. H. Fedynyshyn, R. Sinta, E. Matijevic, *Langmuir* **16**, 9031 (2000).
- [8] M. L. Hans, A.M. Lowman, *Curr. Opin. Solid State Mater. Sci.* **6**, 319 (2002).
- [9] E. Merisko-Liversidge, G. G. Liversidge, E. R. Cooper, *Eur. J. Pharm. Sci.* **18**, 113 (2003).
- [10] K.H. Cho, J.E. Park, T. Osaka, S.G. Park, *Electrochimica Acta* **51**, 956 (2005).
- [11] U. Samuel, J. Guggenbichler, *Int. J. Antimicrob. Agents* **23**, 75 (2004).
- [12] S. Percival, P.G. Bowler and J. Dolman, *Int. Wound J.* **4**, 186 (2007).
- [13] N. Vigneshwaran, A. Kathe, P. Varadarajan, R. Nachane, R. H. Balasubramanya, *J. Nanosci. Nanotechnol.* **7**, 1893 (2009).
- [14] N. Cioffi, N. Ditaranto, L. Torsi, R. Picca, E. De Giglio, L. Sabbatini, L. Novello, G. Tantillo, T. Bleve-Zacheo, P. Zambonin, *Anal. Bioanal. Chem.* **382**, 1912 (2005).
- [15] S. M. Hussain, L. K. Braydich-Stolle, J. L. Speshock, K. O. Yu, A. M. Schrand, C. M. Grabinski, N. M. Schaeublin, R. C. Murdock, A. B. Castle, M. C. Moulton, E. I. Maurer, C.NMI Carlson, S. J. Kunzleman, K. L. Hess, R. L. Jones, AFRL-RH-WP-TR-2009-0044. (2008).
- [16] R. Vaidyanathan, K. Kalishwaralal, S. Gopalram, S. Gurunathan, *Biotechnol Adv.* **27**, 924 (2009).
- [17] S. Moaddab, H. Ahari, D. Shahbazzadeh, A.A. Motallebi, A.A. Anvar, J. Rahman-Nya, M.R. Shokrgozar, *Int. Nano. Lett.* **1**, 11(2011).
- [18] K. Satyavani, S. Gurudeeban, T. Ramanathan, T. Balasubramanian, *J. Nanobiotechnol.* **9**, 2 (2011).
- [19] M. Yoshio, H. Wang, Y.S. Lee, K. Fukuda, *Electrochimica Acta.* **48**, 791 (2003).
- [20] B.J. Wiley, S.H. Im, Z.Y. Li, J. McLellan, A. Siekkinen and Y. Xia, *J. Phys. Chem. B.* **110**, 15666 (2006).
- [21] A.R. Bijanzadeh, M.R. Vakili, R. Khordad, *Internat. J. Phys. Sci.* **7**, 1943 (2012).
- [22] MP Zheng, MY Gu, YP Jin, G. L Jin, *Mater. Res. Bull.* **36**, 853 (2001).
- [23] B.L. He, J.J. Tan, Y.L. Kong and H.F. Liu, *J. Mol. Catal. A: Chem.* **221**, 121(2004).
- [24] J. Huang, G. Zhan, B. Zheng, D. Sun, F. Lu, Y. Lin, H. Chen, Z. Zheng, Y. Zheng, Q. Li, *Ind. Eng. Chem. Res.* **50**, 9095(2011).
- [25] I. Sondi, D. V. Goia, and E. Matijevic, *J. Colloid Inter. Sci.* **260**,75 (2003).
- [26] L. Suber, I. Sondi, E. Matijevic, and D. V. Goia, *J. Colloid Inter. Sci.* **288**, 489 (2005).
- [27] A.I. Al-Ayash, M.T. Wilson, *Biochem J.* **177**, 641(1979).
- [28] L. Suber, W.R Plunkett, *Nanoscale* **2**, 128 (2010).
- [29] D.K. Lee, I.S. Lim, Y.S. Lee , D. H. Reignier, G.H. Jeung, *J. Chem. Phys.* **126**, 244313 (2007).
- [30] A. Panacek, L. Kvitek, R. Prucek, M. Kolar, R. Vecerova, N. Pizurova, V. K. Sharma, T. Nevecna, R. Zboril, *J. Phys. Chem. B.* **110**, 16248 (2006).
- [31] K. Shameli, M. Bin Ahmad, S. D. Jazayeri, P. Shabanzadeh, P. Sangpour, H. Jahangirian, Y. Gharayebi, *Chem. Cent. J.* **6**, 73 (2012).
- [32] Y. Matsumura, K. Yoshikata, S. Kunisaki, T. Tsuchido. *Appl. Environ. Microbiol.* **69**, 4278 (2003).
- [33] S. K. Gogoi, P. Gopinath, A. Paul, A. Ramesh, S.S. Ghosh, A. Chattopadhyay. *Langmuir* **22**, 9322 (2006).
- [34] G. M. Sulaiman, A. A.W. Mohammad, H. E. Abdul-Wahed, M. M. Ismail, *Dig. J. Nanomater. Biostruct.* **8**, 273 (2013).